ELSEVIER

Journal of Molecular Structure (Theochem) 673 (2004) 155–164

THEO CHEM

www.elsevier.com/locate/theochem

Structural, energetic, and electronic properties of $(CH_3CN)_{2-8}$ clusters by density functional theory

R.A. Mata[a,b], B.J. Costa Cabral[a,b,*]

[a]*Departamento de Química e Bioquímica, Faculdade de Ciências da Universidade de Lisboa, 1749-016 Lisboa, Portugal*
[b]*Grupo de Física Matemática da Universidade de Lisboa, Av. Professor Gama Pinto 2, 1649-003 Lisboa, Portugal*

Received 18 September 2003; revised 1 December 2003; accepted 5 December 2003

Abstract

Structural, energetic, and electronic properties of acetonitrile (ACN) clusters $(CH_3CN)_n$, where $n = 2-8$ is the number of ACN molecules, have been investigated by density functional theory. The structure of ACN clusters can be associated with the replica of building units, which may involve dimers, trimers, or tetramers. Two types of building units can be identified: structures that are mainly stabilized by CH···N interactions; structures where dipolar interactions are dominant. We are providing evidence that competition between weak hydrogen bonding and dipolar interactions may determine the structure of ACN clusters. In comparison with typical hydrogen bonding systems (e.g. $(H_2O)_n$, $(HF)_n$), nonadditive polarization effects are much less important. The average monomer dipole moment $\bar{\mu}$ in ACN clusters tends to values in the 4.5–4.7 D range for larger aggregates. This result for $\bar{\mu}$ is in very good agreement with an experimental prediction for the dipole moment of liquid acetonitrile of 4.5 ± 0.1 D [Mol. Phys. 73 (1991) 985].

Keywords: Acetonitrile; Density functional theory; Dipole moment

1. Introduction

Acetonitrile (ACN) is a widely used dipolar aprotic solvent. Like others in its class (e.g. tetrahydrofuran, dimethylformamide, and dimethylsulphoxide), it is able to dissolve a wide variety of hydrophilic and hydrophobic substances while revealing a low acidity. Many applications can be found in organic synthesis, electroorganic, and physical organic chemistry, just to name a few. ACN role as a common solvent in a variety of chemical processes and its unusually high dipole (3.92 D) [1] for such a small organic molecule, has caught the attention of several experimental [2–10] and theoretical [11–26] works.

Some authors have referred to neat acetonitrile as the perfect dipolar system, since strong dipole–dipole interactions should determine most properties in condensed phases. In fact, experimental information seems to support this statement. In the alpha form, a perfectly ordered crystal monoclinic structure, found in a short temperature range around 220 K, a head-to-tail chain of ACN molecules is observed, running alongside four other antiparallel chains [27]. Each ACN unit is thus paired with his two chain neighbours ($\rightarrow\ \rightarrow$) above and below as well with other units in the surroundings ($\uparrow\downarrow$)—a highly dipole–dipole pair stabilized structure. In the liquid phase, only short range-order is clearly observed and X-ray and neutron diffraction studies [28–30] indicate a small antiparallel/parallel ordering of ACN molecules, which is consistent with energetical stabilization due to dipolar interactions. By assuming that the structure of condensed phases is dominated by this type of behavior, finding a good description of dipolar interactions should be enough to describe most properties of the system. This could explain the moderate success of three-site intermolecular potential models [13,14,22] where the methyl group is represented by a single site or pseudoatom (unified atom approach). These models do fail for single particle dynamics, but reproduce reasonably well most of the liquid state thermal and structural properties [22].

There is some evidence on the importance of hydrogen bonding in ACN. This is particularly clear when ACN interacts with good proton donors (e.g. water) [31,32]. ACN

* Corresponding author. Address: Grupo de Física Matemática da Universidade de Lisboa, Av. Professor Gama Pinto 2, 1649-003 Lisboa, Portugal. Tel.: +351-217904728; fax: +351-217954288.
E-mail address: ben@adonis.cii.fc.ul.pt (B.J. Costa Cabral).

0166-1280/$ - see front matter © 2003 Elsevier B.V. All rights reserved.
doi:10.1016/j.theochem.2003.12.011

has two acceptor sites: the lone pair in the N atoms (σ bonding) and the triple π bonding. However, ACN ability as a proton donor is arguable. The only available hydrogens are located in the methyl group, which means we would be dealing with C–H···PA bridges, where PA is a proton acceptor species. The possibility of CH participating in hydrogen bonding has been intensively discussed for decades and it is still controversial [33]. Even so, infrared (IR) and calorimetric studies [7] have provided some indications of hydrogen bonding involving the methyl carbons in ACN. The interaction energies are, however, quite low. Moreover, they stand alone in a vast collection of experimental data on liquid ACN, where there is no glimpse of this kind of hydrogen bonding. Although ACN may be unable to establish true hydrogen bonds involving the methyl group, it seems reasonable to assume that the hydrogen atoms can interact with the N atom, and that CH···N interactions should be taken into account to correctly describe the properties of ACN aggregates.

In the present work we have investigated the structural, energetic, and electronic properties of $(CH_3CN)_n$ clusters ($n = 2–8$ is the number of ACN molecules) by carrying out quantum-mechanical calculations based on density functional theory (DFT). The study of clusters is important for two main reasons: first, by analyzing the dependence of several properties on the cluster size, we can evaluate the importance of many-body nonadditive contributions including polarization effects [34], and discuss what kind of interactions are involved in the energetical stabilization of different isomers; second, clusters are intermediate structures between isolated species and the bulk phases. Thus, it should be expected that some features of larger aggregates and condensed phases are already present in small clusters.

2. Computational details

A wide variety of functionals was applied to the ACN monomer and dimer. The hybrids were Becke's three-parameter functional (B3) [35] with the non-local correlation provided by the Perdew–Wang 91 expression (PW91) [36] or by Lee, Yang and Parr's (LYP) [37]. Barone and Adamo's Becke-style one-parameter functional, using modified Perdew–Wang exchange (MPW1) [38] and PW91 correlation was also used. The non-hybrid was the Perdew and Wang 1991 exchange and gradient-corrected correlation functional (PW91) [36]. Recently, Tsuzuki and Lüthi [39] provided some evidence that the PW91 functional is adequate for predicting the energetics of complexes where dispersion interactions are expected to be important including neon, argon, and hydrogen bonded complexes. A recent application to HCl clusters [34] supports this conclusion. For completeness, results based on the local spin density approximation (SVWN) [40] are also reported, although it is known that this approximation is inadequate to model this kind of system.

For $n = 3$ and $n = 4$, only three functionals were employed (PW91, MPW1PW91 and B3LYP). Optimizations from $n = 5$ to 8 were performed with the B3LYP hybrid. The basis set used for the geometry optimizations was Dunning's correlation consistent polarized valence double zeta (cc-pVDZ) [41]. To analyze the dependence of the optimized structures on the introduction of diffuse functions, for some clusters, geometry optimizations with the aug-cc-pVDZ basis set [42] were also carried out. All geometries have been fully optimized without any symmetry constraint.

Single-point energy calculations on the optimized structures were carried out using augmented basis sets of double (aug-cc-pVDZ) and triple valence (aug-cc-pVTZ) [42]. Frequency calculations were carried out for all optimized structures, confirming them as local minima on the potential energy surface.

Interaction energies were estimated using the supermolecular approach [43]. The binding energy of a cluster with n monomers $\Delta E_{0,n}$ is defined as:

$$\Delta E_{0,n} = E_0[(CH_3CN)_n] - nE_0[(CH_3CN)]$$

The stepwise binding energy $\Delta E_{0,n,n-1}$ for the same cluster is given by:

$$\Delta E_{0,n,n-1} = E_0[(CH_3CN)_n] - E_0[(CH_3CN)_{n-1}] - E_0[(CH_3CN)]$$

The analogue quantities $\Delta E_{e,n}$ and $\Delta E_{e,n,n-1}$ do not include the zero-point vibrational energy corrections. These quantities were corrected for basis set superposition error (BSSE) when using cc-pVDZ or aug-cc-pVDZ basis sets. The BSSE was estimated to be low on aug-cc-pVTZ calculations and was therefore neglected. The counterpoise method of Boys and Bernardi [44] was used, including the fragment relaxation energies contributions [45].

By adding thermal corrections at a temperature T (in K) to $\Delta E_{0,n}$, and $\Delta E_{0,n,n-1}$, respectively, we define the binding enthalpy, $\Delta H_{0,n}$, and the stepwise binding enthalpy, $\Delta H_{0,n,n-1}$. When $n = 2$, $\Delta H_{0,2} \equiv \Delta H_{0,2,1}$, and these quantities will be represented as $\Delta H_{2,T}$.

Charge polarization in ACN clusters has been analyzed by fitting atomic charges to the electrostatic potential on van der Waals surfaces [46,47]. From these charges (Merz–Kollman–Singh ≡ MKS charges), we have estimated the average monomer dipole moment, $\bar{\mu}$, in ACN clusters. All calculations were performed using the GAUSSIAN98 [48] program.

3. Results and discussion

3.1. Monomer and dimer

The experimental monomer geometry is well known in the gas [49] and in the liquid phase [29]. Notably, it does not

Table 1
Structural properties and dipole moment for the acetonitrile molecule

	B3LYP	B3PW91	MPW1PW91	PW91	SVWN	MP2[a]	Experiment[b]
r(C–N)	1.161	1.161	1.159	1.172	1.167	1.181	1.157
r(C–C)	1.462	1.456	1.454	1.459	1.441	1.464	1.458
r(C–H)	1.101	1.100	1.098	1.106	1.109	1.093	1.102
Θ(H–C–C)	110.2	110.1	110.1	110.4	109.0	110.5	109.5
μ[c]	4.05	4.05	4.06	4.01	4.12	3.98	3.92[d]

Geometries optimized with the cc-pVDZ basis set. Distances in Å. Angles in degrees. Dipoles in D.
[a] MP2/6-31 + G(d) calculation. From Ref. [21].
[b] From Ref. [49].
[c] DFT dipoles were calculated with the aug-cc-pVDZ basis set.
[d] From Ref. [1].

seem to suffer great change. Structural parameters and dipole moments for the ACN molecule are reported in Table 1, where they are compared with experimental data [49], and with predictions from other theoretical studies [21].

For the ACN monomer, geometries from hybrid functionals are in excellent agreement with experiment. PW91 and MP2 slightly overestimate the C–N bond length. Overall, all theoretical methods predict structural properties for the monomer in very good agreement with experiment. The gas phase dipole moments (μ) are also in very good agreement with experiment (3.92 D) [1].

The optimized geometries for the ACN antiparallel and linear dimers are shown in Fig. 1. Table 2 reports results for the antiparallel dimer structure. Apparently, no experimental data for the dimer structure is available. For the antiparallel dimer, all methods predict a C···C intercarbon distance of ~3.4 Å. The intermolecular N···H distance ranges from 2.469 (PW91) to 2.568 Å (B3PW91). Comparison between the geometries of the isolated monomer and the monomer geometry in the dimer shows no significant change. Intramolecular distances in $(CH_3CN)_{2-8}$ clusters differ by less than 0.005 Å. Valence angles are similar within one degree. This feature indicates that optimizations of larger acetonitrile clusters could be carried out by freezing the monomers geometry, although we have not adopted such a procedure. For the antiparallel dimer B3LYP/aug-cc-pVDZ and B3LYP/cc-pVDZ optimized structures are very similar (Fig. 1). This indicates that geometric parameters of ACN aggregates may not significantly change on the inclusion of diffuse functions.

Despite the fact that, for pure dipoles, the head-to-tail linear arrangement is the most energetically stable structure, some theoretical studies at a correlated quantum-mechanical level, have only reported the antiparallel ACN dimer as a local energy minimum [21,23]. Attention should be reverted to the work by Popelier et al. [15], the first to mention this configuration. They provided a PES plot where it could be seen that this dimer had a very small barrier for conversion to the global minimum [15]. The PES surface could be quite flat and some theoretical levels may not predict the correct form, leading to one small imaginary frequency. Very recently, the structure of the linear dimer has been optimized at the MP2/6-311 + G(d) level by Nguyen and Peslherbe [26]. Experimental evidence for the collinear isomer of the acetonitrile dimer has been provided

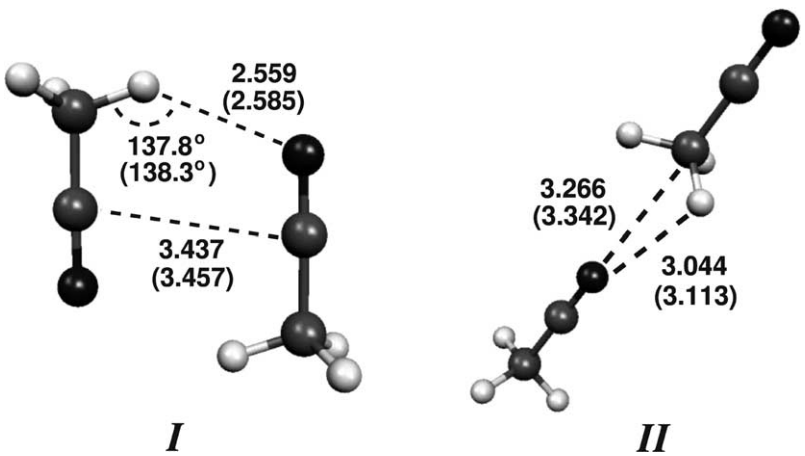

Fig. 1. Optimized structures of the ACN dimers. Angles (in degrees) and intermolecular distances (in Å) are presented for B3LYP optimizations with the cc-pVDZ and (aug-cc-pVDZ) basis sets. Antiparallel isomer I is found to be more stable than the linear isomer II by ~8 kJ mol^{-1}.

Table 2
Structural properties for the acetonitrile antiparallel dimer

	B3LYP	B3PW91	MPW1PW91	PW91	SVWN	MP2[a]
r(N···H)	2.559	2.568	2.526	2.469	2.185	2.568
r(C···C)[b]	3.437	3.449	3.398	3.367	3.096	3.368
Θ(C–H···N)	137.8	138.3	137.7	138.2	137.0	132.9

Geometries optimized with the cc-pVDZ basis set. Distances in Å. Angles in degrees.
[a] MP2/6-31 + G(d) calculation. From Ref. [21].
[b] r(C···C) is the intermolecular carbon–carbon distance (Fig. 1).

by Dessent et al. [8]. The B3LYP/cc-pVDZ optimized structure for the ACN linear dimer is shown in Fig. 1. The N···H distance is 3.04 Å, indicating that no CH···N hydrogen bonding is involved in the energetical stabilization of this structure. A B3LYP/aug-cc-pVDZ geometry optimization of the linear dimer confirmed it as a minimum, providing, however, larger intermolecular distances (Fig. 1). This may be attributed to the fact that the collinear dimer structure is determined by dipolar head-to-tail interactions. It shows some dependence on the introduction of diffuse functions possibly due to electronic delocalization related to polarization along the C–N axis. Still, we have some indications that the inclusion of diffuse functions should not greatly change the geometric parameters of larger aggregates (see also caption of Fig. 2).

Through frequency calculations on the optimized structures, harmonic intermolecular frequencies are available as well. They are located under the lowest measured frequency for the monomer (around 360 cm^{-1}) [3]. Intermolecular frequencies for the ACN antiparallel dimer are reported in Table 3, where they are compared with Knözinger and Leutloff results [2], which are from IR measurements in a rare gas matrix preparation. Semi-quantitative agreement is obtained between our results and these experiments. Frequencies predicted by hybrid functionals are underestimated. This is worsened by the fact that these values are under an harmonic approximation, which overestimates the frequencies. The modes close to 124 and 105 cm^{-1} correspond to methyl hydrogen libration and twisting mode of the two monomer units, respectively. In a recent study, Cabaleiro-Lago et al. [21] carried out geometry optimizations at the B3LYP/6-31 + G(d) level. Their calculated frequencies (85, 84, 81, 78, 71 and 40 cm^{-1}) were in poor agreement with experiment, probably due to the basis set employed. This seems to be confirmed by the MP2(FC)/cc-pVDZ results also reported in Table 3, which are slightly improved over the MP2/6-31 + G(d) predictions (116, 105 cm^{-1}) reported in the same study [21].

Binding energies for the ACN dimer ($\Delta E_{e,2}$ and $\Delta E_{0,2}$) are presented in Table 4, where BSSE corrections are also reported. These corrections are significant (~30% of the uncorrected values) when binding energies are calculated with the cc-pVDZ basis set, while the aug-cc-pVDZ values are only mildly affected (~6%). Thus, cc-pVDZ interaction energies are unreliable for the discussion of the energetical properties of ACN clusters. In agreement with several theoretical predictions [15,26], we find that the antiparallel dimer of acetonitrile is the most stable structure. At the PW91/aug-cc-pVTZ//PW91/cc-pVDZ level,

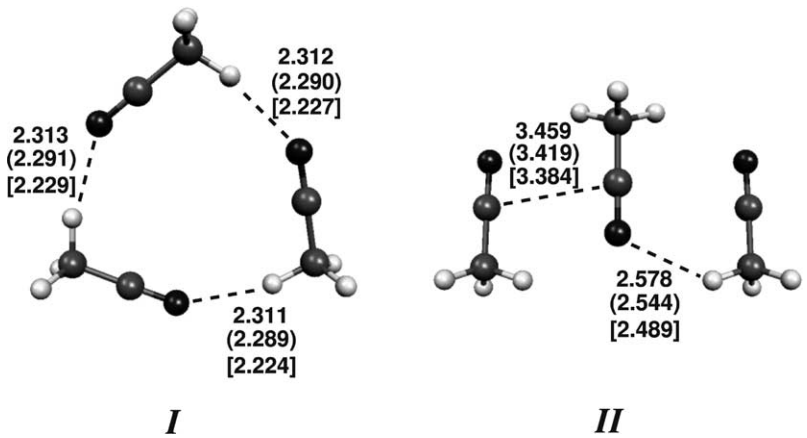

Fig. 2. Optimized structures of the ACN trimers. Intermolecular distances (in Å) are from B3LYP, (MPW1PW91), and [PW91] calculations with the cc-pVDZ basis set. The cyclic isomer I is stabilized by CH···N interactions. Isomer II involves antiparallel dipolar interactions. A B3LYP/aug-cc-pVDZ calculation predicts that the distances are 2.341, 2.339 and 2.334 Å, illustrating that the optimized structures are not significantly dependent on the introduction of diffuse functions.

Table 3
Intermolecular frequencies (in cm^{-1}) for the acetonitrile dimer

B3LYP	B3PW91	MPW1PW91	PW91	SVWN	MP2[a]	Experiment[b]
108.5, 102.6	107.6, 99.0	112.1, 104.4	121.6, 111.7	172.5, 161.0	122.5, 109.5	124, 105
99.6, 98.7	94.4, 92.2	103.4, 99.9	111.0, 107.9	160.7, 141.4		
79.8, 43.0	75.6, 42.1	80.8, 40.0	86.1, 43.8	120.3, 53.3		

Geometries optimized with the cc-pVDZ basis set.
[a] MP2(FC)/cc-pVDZ frequencies.
[b] ACN dimer in Ar matrix. From Ref. [2].

$\Delta E_{e,2} = -21.9$ kJ mol^{-1}, which is in excellent agreement with the MP2/6-311 + G(d) calculation reported by Ford and Glasser (-21.0 kJ mol^{-1}) [23]. The energy difference between the antiparallel and linear dimer ranges from -7.9 (B3LYP/aug-cc-pVTZ//B3LYP/cc-pVDZ) to -10.1 kJ mol^{-1} (PW91/aug-cc-pVTZ//PW91/cc-pVDZ). These results are in good agreement with the CCSD(T)/6-311 + G(2df,pd)//MP2/6-311 + G(d) value of Nguyen and Peslherbe (-9.2 kJ mol^{-1}) [26].

Binding enthalpies are also reported in Table 4, where they are compared with the most recent experimental result ($\Delta H_2 = -20.9 \pm 0.5$ at $T = 360$ K) [4,5]. Some significant

Table 4
Binding energies and dimerization enthalpies (in kJ mol^{-1}) for acetonitrile dimers

	Isomer I			Isomer II		
	$\Delta E_{e,2}$	$\Delta E_{0,2}$	BSSE	$\Delta E_{e,2}$	$\Delta E_{0,2}$	BSSE
B3LYP/cc-pVDZ	−15.0	−11.6	6.5	−7.6	−6.6	3.7
aug-cc-pVDZ[a]	−16.8	–	1.6	−8.7	–	1.5
aug-cc-pVTZ[a]	−17.2	–	–	−9.3	–	–
B3PW91/cc-pVDZ	−12.9	−9.8	5.1			
aug-cc-pVDZ[b]	−14.3	–	1.3			
aug-cc-pVTZ[b]	−14.5	–	–			
MPW1PW91/cc-pVDZ	−16.8	−13.5	5.4	−8.3	−7.5	3.0
aug-cc-pVDZ[c]	−18.2	–	1.3	−9.3	–	1.3
aug-cc-pVTZ[c]	−18.2	–	1.3	−9.8	–	–
PW91/cc-pVDZ	−19.9	−16.4	7.3	−9.7	−8.9	4.2
aug-cc-pVDZ[d]	−21.7	–	1.6	−11.2	–	1.5
aug-cc-pVTZ[d]	−21.9	–	–	−11.8	–	–
SVWN/cc-pVDZ	−38.2	−34.1	8.2			
aug-cc-pVDZ[e]	−41.0	–	2.4			
aug-cc-pVTZ[e]	−41.2	–	–			
MP2/6-311 + G(d)[f]	−21.0	–	–			
6-31++G(d,p)[g]	−20.8	–	5.6			
	$\Delta H_{2,298}$	$\Delta H_{2,360}$				
B3LYP/aug-cc-pVDZ[a]	−11.9	−11.0				
B3PW91/aug-cc-pVDZ[b]	−9.3	−8.3				
MPW1PW91/aug-cc-pVDZ[c]	−13.0	−12.0				
PW91/aug-cc-pVDZ[d]	−16.8	−15.8				
SVWN/aug-cc-pVDZ[e]	−36.6	−35.6				
MP2/6-31 + G(d)[h]	−15.1	–				
Experiment[i]	–	-20.9 ± 0.5				

Results from aug-cc-pVTZ calculations are not corrected for BSSE.
[a] Geometry optimized at B3LYP/cc-pVDZ.
[b] Geometry optimized at B3PW91/cc-pVDZ.
[c] Geometry optimized at MPW1PW91/cc-pVDZ.
[d] Geometry soptimized at PW91/cc-pVDZ.
[e] Geometry optimized at SVWN/cc-pVDZ.
[f] From Ref. [23].
[g] From Ref. [16].
[h] From Ref. [21].
[i] Determined by thermal conductivity experiments in a temperature range of 338–387 K [5].

deviations from experiment ($\sim 5-12$ kJ mol^{-1}) can be observed. The best agreement with experiment is from the PW91 calculation (-15.8 kJ mol^{-1}).

3.2. Trimer and tetramer

3.2.1. Trimer

Fig. 2 shows the optimized structures for the ACN trimers. Structure I is a cyclic structure, which involves three equivalent CH···N interactions. In this case, dipolar interactions apparently play a minor role. The N···H distance is ~ 2.29 Å (MPW1PW91/cc-pVDZ). The second trimer II is clearly stabilized by antiparallel dipolar interactions. Isomer II can be viewed as a dimer, to which one antiparallel monomer has been added to one side. The intermolecular distances (Fig. 2) are similar to those found in the dimer. For example, CH···N ~ 2.6 Å. The N···H distances are slightly dependent on the functional and PW91 affords the shortest. However, for isomer I, they are in the typical range of distances involving CH as a potential proton donor (~ 2.3 Å) [33].

Results for the trimer binding energies are reported in Table 5. Isomer I is the most stable by ~ 9 kJ mol^{-1} (the three functionals agree quite well on this difference).

Table 5
Binding energies (in kJ mol^{-1}) for the acetonitrile trimers

	Isomer I	Isomer II
B3LYP/cc-pVDZ		
$\Delta E_{e,3}$	−36.5	−26.9
$\Delta E_{0,3}$	−29.2	−20.8
BSSE	13.9	12.7
B3LYP/aug-cc-pVDZ[a]		
$\Delta E_{e,3}$	−38.5	−29.9
BSSE	3.9	3.2
B3LYP/aug-cc-pVTZ[a]		
$\Delta E_{e,3}$	−39.7	−30.6
MPW1PW91/cc-pVDZ		
$\Delta E_{e,3}$	−39.5	−30.1
$\Delta E_{0,3}$	−32.4	−24.3
BSSE	11.7	10.7
MPW1PW91/aug-cc-pVDZ[b]		
$\Delta E_{e,3}$	−40.4	−32.5
BSSE	3.4	2.7
PW91/cc-pVDZ		
$\Delta E_{e,3}$	−46.3	−36.3
$\Delta E_{0,3}$	−38.9	−30.2
BSSE	15.9	14.4
PW91/aug-cc-pVDZ[c]		
$\Delta E_{e,3}$	−48.0	−39.5
BSSE	4.0	3.2

[a] Geometry optimized at B3LYP/cc-pVDZ.
[b] Geometry optimized at MPW1PW91/cc-pVDZ.
[c] Geometry optimized at PW91/cc-pVDZ.

This isomer, as above stated, should be mostly stabilized by CH···N interactions. Dipole pairing is of reduced significance due to the deterrent relative orientation of the monomers (although it does contribute to the overall binding energy). The fact that isomer I has a larger (or at least comparable) binding energy than II was partly expected. Dipole paired structures with an odd number of monomers should be a little destabilized. Other interactions can be therefore of particular significance in these structures. It is not possible, however, to assure that isomer I will be the global minimum. No thorough investigation of the potential surface was performed. Our main objective is to investigate how the different structural features reflect different types of interactions that determine the properties of ACN clusters. Other local minima have been proposed [15,16].

3.2.2. Tetramer

Fig. 3 shows three acetonitrile tetramers. Structure I is a cyclic tetramer. To our knowledge, it has not been mentioned in earlier theoretical studies. It presents four similar N···H distances of 2.27 Å (MPW1PW91/cc-pVDZ), which are slightly shorter in comparison with the trimer I (2.29 Å), but in this case, C–H···N angles are almost linear, thanks to an affordable larger ring.

The other structures (II and III) correspond to two different possibilities for duplicating the dimer arrangement. The structure referred to as II displays alternated pairing, while in III every monomer is paired to two others in the cluster. Again, the intermolecular distances agree well with those found in the dimer.

Table 6 reports the binding energies for the acetonitrile tetramers. At the B3LYP/aug-cc-pVTZ//B3LYP/cc-pVTZ level, the cyclic structure I is more stable than the two others by less than 4 kJ mol^{-1}. Surprisingly enough, all three structures present quite similar energies. This is of some significance, since in this case we are not dealing with an odd number of monomers. Dipole paired structures can be built from layers of pairing dimers, which are found to be extremely stable. Even so, structure I is able to rival with both, while presenting structural data consistent with weak hydrogen bonding. This supports our initial assumption about the relevance of other intermolecular interactions in addition to the dipolar ones, even if isomer I is not the global minimum.

3.3. Clusters up to $n = 8$

3.3.1. Structure and energetics

The initial geometries for clusters from $n = 5$ up to 8 were obtained through Monte Carlo simulated annealing by using a pairwise additive intermolecular potential [12]. These structures were then reoptimized with the B3LYP functional. They are presented in Fig. 4 and show both tendencies earlier discussed, dipolar and CH···N interactions. The pentamer is similar to a distorted tetramer

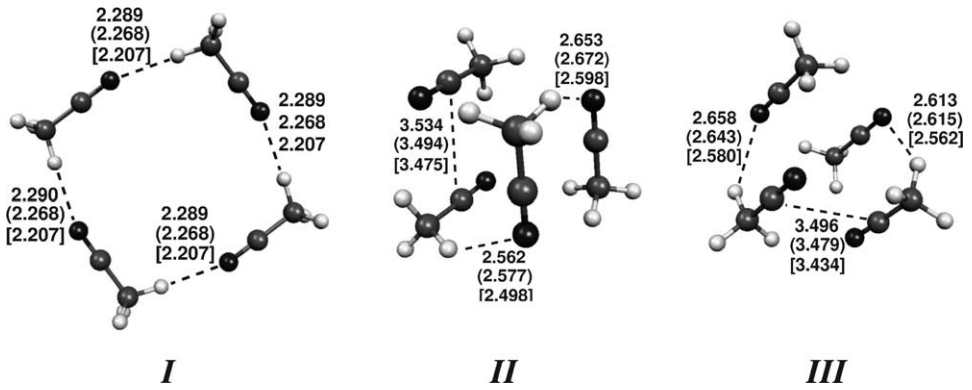

Fig. 3. Optimized structures of the ACN tetramers. Intermolecular distances (in Å) are from B3LYP, (MPW1PW91), and [PW91] calculations with the cc-pVDZ basis set.

(isomer II), to which is added one monomer. The hexamer is particularly interesting as it resembles two trimers (isomer I), one on top of the other. The heptamer and octamer are more difficult to describe based on smaller structures, but also show some of the discussed patterns.

Since dispersion interactions are not correctly accounted for in the B3LYP functional, it should be evaluated how this may be significant on the optimization of these larger clusters. As stated earlier, PW91 should take into account this effect. By comparing structures up to $n = 4$, although PW91 predicts lower intermolecular distances (which cannot be solely attributed to the dispersion interaction effect), the geometries are for most purposes similar.

Binding energies for the complete series (from $n = 2$ up to 8) are reported in Table 7 and represented in Fig. 5. The isomers chosen for $n = 3$ and 4 were the structures I, which are the most stable isomers. The results for the binding energies seem to suggest only a slight cooperative effect and Fig. 5 shows an almost linear behavior of the binding energy as a function of the number of monomers n. Stepwise binding energies ($\Delta E_{e,n,n-1}$) reported in Table 7 support this statement, exception made to $n = 7$. Its stepwise binding energy is smaller, which could indicate a low energy gain when adding a ACN molecule to the hexamer cluster. Although a similar effect can be observed when we add an ACN molecule to the ACN tetramer, it is unlikely for cooperative effects to only be seen when going from 6 to 7 monomers. As the size increases, these effects tend to level off. The most likely explanation is that the optimized cluster (for $n = 7$) is a local minimum located high above the global. In fact, our procedure was based on the assumption that as we progressed through the series the number of isomers would increase, but their energies would lie in a small range.

As for the observed small cooperative effects they can be explained as follows. The major intermolecular forces involved seem to be dipole pairing and a weak interaction between methyl hydrogens and the N lone electron pair. These interactions should only slightly disturb each monomer unit. The possibility of hydrogen bonding was raised but is quite questionable. No significant changes were observed in the bond distances and on the vibrational spectra. Also the distance between the methyl carbon (bonded to the interacting hydrogen) and the N atom lies slightly above the sum of the van der Waals radii (3.25 Å). The closest observed values in the clusters were ~3.36 Å. Although these are only a few of many tests used when checking for hydrogen bonding, they do place serious doubts on its existence. The CH···N interactions lie at most on the dubious border of weak hydrogen bonding [33].

Table 6
Binding energies (in kJ mol^{-1}) for the acetonitrile tetramers

	Isomer I	Isomer II	Isomer III
B3LYP/cc-pVDZ			
$\Delta E_{e,4}$	−52.7	−46.0	−45.4
$\Delta E_{0,4}$	−42.4	−35.8	−34.5
BSSE	19.5	24.5	24.2
B3LYP/aug-cc-pVDZ[a]			
$\Delta E_{e,4}$	−54.9	−51.4	−50.6
BSSE	5.8	6.7	6.9
B3LYP/aug-cc-pVTZ[a]			
$\Delta E_{e,4}$	−57.3	−53.1	−52.3
MPW1PW91/cc-pVDZ			
$\Delta E_{e,4}$	−56.6	−51.3	−51.2
$\Delta E_{0,4}$	−46.6	−42.0	−41.7
BSSE	16.2	20.8	20.3
MPW1PW91/aug-cc-pVDZ[b]			
$\Delta E_{e,4}$	−57.4	−55.8	−55.4
BSSE	5.3	5.6	5.4
PW91/cc-pVDZ			
$\Delta E_{e,4}$	−65.5	−64.2	−63.8
$\Delta E_{0,4}$	−55.2	−54.2	−52.6
BSSE	22.1	27.5	27.3
PW91/aug-cc-pVDZ[c]			
$\Delta E_{e,4}$	−67.5	−69.8	−69.0
BSSE	6.0	6.7	7.0

[a] Geometry optimized at B3LYP/cc-pVDZ.
[b] Geometry optimized at MPW1PW91/cc-pVDZ.
[c] Geometry optimized at PW91/cc-pVDZ.

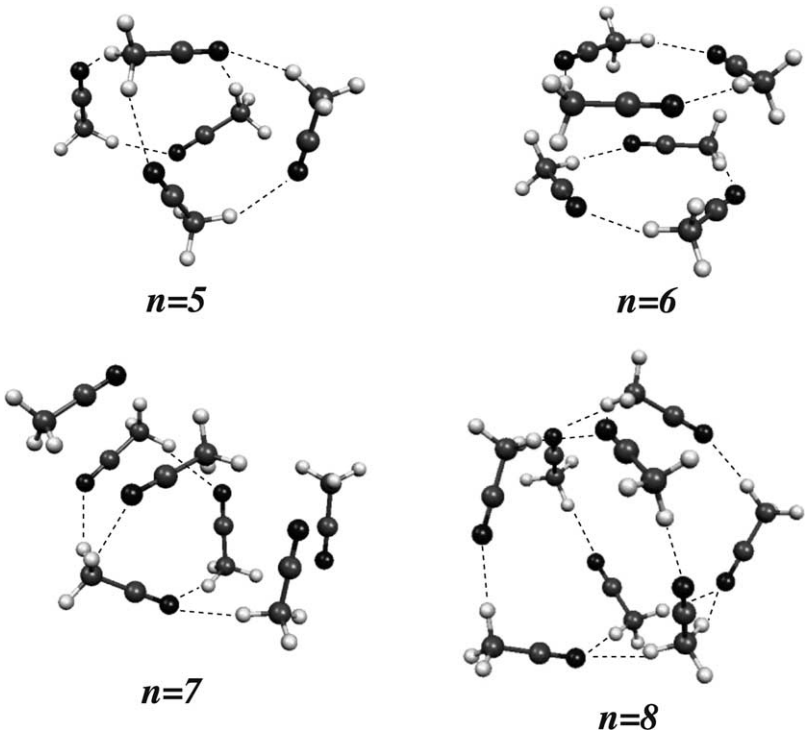

Fig. 4. B3LYP/cc-pVDZ optimized structures of the $(CH_3CN)_{5-8}$ clusters. CH···N distances are represented by dashed lines when they are less than 2.5 Å.

Nevertheless, they seem to play an important role as the N lone pair will most probably be stabilized by approaching a hydrogen atom, even if only slightly polarized. Furthermore, it is clear on the dipole paired structures that the methyl groups are oriented towards the N atoms.

3.3.2. Polarization effects

Although nonadditive polarization effects are apparently not very relevant in determining the structural and energetic properties of ACN clusters, it is important to investigate how the electronic properties of the clusters, particularly the charge distribution, depend on the cluster size. We have evaluated the average monomer dipole moment $\bar{\mu}$ for the different clusters by using the charges fitted to the electrostatic potential. The results are presented in Fig. 6. There is some enhancement of the dipolar moment as the cluster size increases, but the range of values is not very large (4.0–4.7 D). For $n > 4$, the values apparently cease to increase and tend to values in the 4.5–4.7 D range. This means an increase of ~16% relative to the gas phase dipole at the same theoretical level (4.05 D). An experimental value of 4.5 ± 0.1 D [6] has been proposed for the acetonitrile dipole moment in the liquid. This value, which is based on the relationship between far-IR optical constants of the liquid and the dipole moment [6] compares well to our result. Even more if we take into account that our theoretical prediction for the dipole moment in the gas phase (4.05 D) overestimates in about 0.1 D the experimental

Table 7
Binding energies (in kJ mol^{-1}) for $(CH_3CN)_{2-8}$ clusters

	2	3	4	5	6	7	8
B3LYP/cc-pVDZ							
$\Delta E_{0,n}$	−11.6	−29.2	−42.4	−50.3	−68.8	−73.5	−97.9
$\Delta E_{e,n}$	−15.0	−36.5	−52.7	−63.8	−87.0	−94.1	−122.1
$\Delta E_{e,n,n-1}$	−15.0	−21.5	−16.2	−11.0	−23.3	−7.1	−27.9
BSSE	6.5	13.9	19.5	29.6	41.5	49.2	49.7
B3LYP/aug-cc-pVDZ[a]							
$\Delta E_{e,n}$	−16.8	−38.5	−54.9	−68.1	−93.1	−102.1	−127.4
$\Delta E_{e,n,n-1}$	−16.8	−21.7	−16.4	−13.2	−25.0	−8.9	−25.4
BSSE	1.6	3.9	5.8	8.9	12.5	15.6	16.6
B3LYP/aug-cc-pVTZ[a]							
$\Delta E_{e,n}$	−18.4	−42.3	−60.7	−77.0	−105.6	−117.6	−144.0
$\Delta E_{e,n,n-1}$	−18.4	−23.9	−18.3	−16.3	−28.6	−12.0	−26.3

For $n = 2$–4 the most stable isomers have been selected.
[a] Geometry optimized at B3LYP/cc-pVDZ.

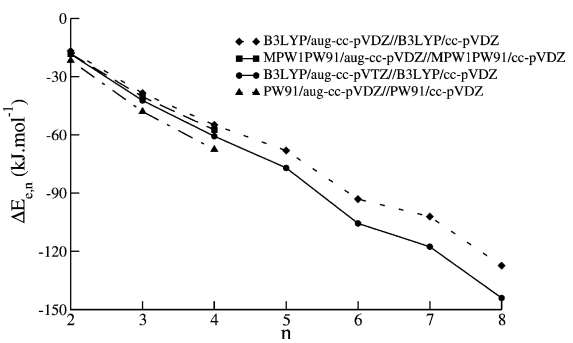

Fig. 5. Binding energy $\Delta E_{e,n}$ (in kJ mol^{-1}) for ACN clusters as a function of the cluster size n from $n = 2$–8. Results are from single-point energy calculations based on cc-pVDZ optimized structures.

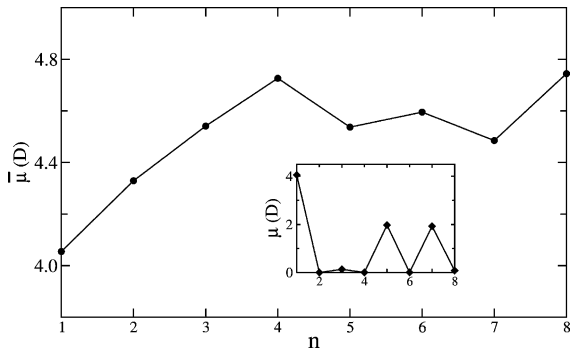

Fig. 6. Average monomer dipole moment $\bar{\mu}$ (in D) for ACN clusters as a function of the number of monomers n. The inset shows the total dipole moment μ. The results are from B3LYP/aug-cc-pVDZ//B3LYP/cc-pVDZ calculations.

value [1]. It is interesting to compare the increase of the dipole moment in ACN clusters (~16%) with the significant enhancement of the dipole moment in water clusters (~40%) [50,51]. Since the increase of the water dipole moment is a clear signature of polarization effects induced by hydrogen bonding it seems reasonable to conclude that these effects are much less important in the present case of a strong dipolar fluid such as acetonitrile.

4. Conclusions

DFT calculations have been performed on acetonitrile clusters up to a maximum size of eight molecules. The performance of various functionals was tested by comparing results for the monomer and dimer with those obtained by experiment and earlier theoretical studies. The hybrid functionals seem to slightly underestimate the dimerization energy when compared to ab initio correlated methods and the experimental estimate. This should arise possibly from their inability to account for dispersion interactions. The PW91 functional affords the best agreement.

For the trimer and the tetramer, isomers were studied to evaluate the importance of hydrogen bonding (CH···N) and dipole pairing. Our results seem to indicate that these are competing factors in determining the geometry of the free clusters. Dipole–dipole interactions, although being major contributors to the stabilization of these structures, should not be able alone to account for the properties of acetonitrile aggregates. Weak N···H interactions play a significant role in the energetical stabilization of acetonitrile clusters, being found in all of our larger clusters. We emphasize that this conclusion puts some limitations on models for ACN that are simply based on dipolar interactions.

Dipole moments for the monomer and higher order structures were calculated and compare well with the available experimental data. They confirm an increase in ACN polarization of about 16% on going from gas to the condensed phase, which reveals a mild inductive effect when it is compared with polarization effects in typical hydrogen bonding systems.

Acknowledgements

This work was partially supported by the Sapiens program of the FCT, Portugal (Grant No. POCTI/43315/-QUI/2001).

References

[1] P.A. Steiner, W. Gordy, J. Mol. Spectrosc. 21 (1966) 291.
[2] E. Knözinger, D. Leutloff, J. Chem. Phys. 74 (1981) 4812.
[3] Y. Koga, S. Kondo, S. Saeki, W.B. Person, J. Phys. Chem. 88 (1984) 3152.
[4] L.A. Curtiss, M. Blander, Chem. Rev. 88 (1988) 827.
[5] T.A. Renner, M. Blander, J. Phys. Chem. 81 (1977) 857.
[6] T. Ohba, S. Ikawa, Mol. Phys. 73 (1991) 985.
[7] A.A. Stolov, D.I. Kamalova, M.D. Borisover, B.N. Solomonov, Spectrochim. Acta A 50 (1994) 145.
[8] C.E.H. Dessent, J. Kim, M.A. Johnson, J. Phys. Chem. 100 (1996) 12.
[9] T. Takamuku, M. Tabata, A. Yamaguchi, J. Nishimoto, M. Kumamoto, H. Wakita, T. Yamaguchi, J. Phys. Chem. B 102 (1998) 8880.
[10] J.G. Siebers, U. Buck, T.A. Beu, Chem. Phys. 111 (1999) 2436.
[11] D. Wright, M.S. El-Shall, J. Chem. Phys. 100 (1994) 3791.
[12] H.J. Böhm, I.R. McDonald, P.A. Madden, Mol. Phys. 49 (1983) 347.
[13] W.L. Jorgensen, J.M. Briggs, Mol. Phys. 63 (1988) 547.
[14] D.M.F. Edwards, P.A. Madden, I.R. McDonald, Mol. Phys. 51 (1984) 1141.
[15] P.L.A. Popelier, A.J. Stone, D.J. Wales, Faraday Discuss. 97 (1994) 243.
[16] E.M. Cabaleiro-Lago, M.A. Ríos, J. Phys. Chem. A 101 (1997) 8327.
[17] J.G. Siebers, U. Buck, T.A. Beu, Chem. Phys. 239 (1998) 549.
[18] E.M. Cabaleiro-Lago, M.A. Ríos, Mol. Phys. 96 (1999) 309.
[19] J. Richardi, P.H. Fries, H. Krienke, Mol. Phys. 96 (1999) 1411.
[20] X. Grabuleda, C. Jaime, P.A. Kollman, J. Comput. Chem. 21 (2000) 901.
[21] E.M. Cabaleiro-Lago, J.M. Hermida-Ramón, A. Peña-Gallego, E. Martínez-Núñez, A. Fernández-Ramos, J. Mol. Struct. (Theochem) 498 (2000) 21.
[22] E. Guàrdia, R. Pinzón, J. Casulleras, M. Orozco, F.J. Luque, Mol. Simul. 26 (2001) 287.
[23] T.A. Ford, L. Glasser, Int. J. Quantum Chem. 84 (2001) 226.
[24] A.K. Sum, S.I. Sandler, R. Bukowski, K. Szalewicz, J. Chem. Phys. 116 (2002) 7627.
[25] E.S. Kryachko, M.T. Nguyen, J. Phys. Chem. B 106 (2002) 4267.
[26] T.-N.V. Nguyen, G.H. Peslherbe, J. Phys. Chem. A 107 (2003) 1540.
[27] M. Barrow, Acta Crystallogr. B 37 (1981) 2239.
[28] H. Bertagnolli, P. Chieux, M.D. Zeidler, Mol. Phys. 32 (1976) 1731.
[29] H. Bertagnolli, P. Chieux, M.D. Zeidler, Mol. Phys. 32 (1976) 759.
[30] H. Bertagnolli, M.D. Zeidler, Mol. Phys. 35 (1978) 177.
[31] D. Jamroz, J. Stangret, J. Lingdren, J. Am. Chem. Soc. 115 (1993) 6165.
[32] J.E. Bertie, Z.D. Lan, J. Phys. Chem. B 101 (1997) 4111.
[33] S. Scheiner, Hydrogen Bonding: A Theoretical Perspective, Oxford University Press, New York, 1997.
[34] R.C. Guedes, P.C. do Couto, B.J. Costa Cabral, J. Chem. Phys. 118 (2003) 1272.
[35] A.D. Becke, J. Chem. Phys. 98 (1993) 5648.
[36] J.P. Perdew, Y. Wang, Phys. Rev. B 45 (1992) 13244.
[37] C. Lee, W. Yang, R.G. Parr, Phys. Rev. B 37 (1988) 785.
[38] C. Adamo, V. Barone, J. Chem. Phys. 108 (1998) 664.

[39] S. Tsuzuki, H.P. Lüthi, J. Chem. Phys. 114 (2001) 3949.
[40] S.H. Vosko, L. Wilk, M. Nusair, Can. J. Phys. 58 (1980) 1200.
[41] D.E. Woon, T.H. Dunning Jr., J. Chem. Phys. 98 (1993) 1358.
[42] R.A. Kendall, T.H. Dunning Jr., R.J. Harrison, J. Chem. Phys. 96 (1992) 6796.
[43] F.B. van Duijneveldt, J.G.C.M. van Duijneveldt-van de Rijdt, J.H. van Lenthe, Chem. Rev. 94 (1994) 1873.
[44] S.F. Boys, F. Bernardi, Mol. Phys. 19 (1970) 553.
[45] S. Xantheas, J. Chem. Phys. 104 (1996) 8821.
[46] U.C. Singh, P.A. Kollman, J. Comput. Chem. 5 (1984) 129.
[47] B.H. Besler, K.M. Merz Jr., P.A. Kollman, J. Comput. Chem. 11 (1990) 431.
[48] M.J. Frisch, G.W. Trucks, H.B. Schlegel, G.E. Scuseria, M.A. Robb, J.R. Cheeseman, V.G. Zakrzewski, J.A. Montgomery, R.E. Stratman, J.C. Burant, S. Dapprich, J.M. Millam, A.D. Daniels, K.N. Kudin, M.C. Strain, O. Frakas, J. Tomasi, V. Barone, M. Cossi, R. Cammi, B. Mennucci, C. Pomelli, C. Adamo, S. Clifford, J. Ochterski, G.A. Petersson, P.Y. Ayala, Q. Cui, K. Morokuma, D.K. Malick, A.D. Rabuck, K. Raghavachari, J.B. Foresman, J. Cioslowski, J.V. Ortiz, B.B. Stefanov, G. Liu, A. Liashenko, P. Piskorz, I. Komaromi, R. Gomperts, R.L. Martin, D.J. Fox, T. Keith, M.A. Al-Laham, C.Y. Peng, A. Nanayakkara, C. Gonzalez, M. Challacombe, P.M.W. Gill, B.G. Johnson, W. Chen, M.W. Wong, J.L. Andres, M. Head-Gordon, E.S. Replogle, J.A. Pople, GAUSSIAN-98, Gaussian Inc, Pittsburgh, PA, 1998.
[49] C.C. Costain, J. Chem. Phys. 29 (1958) 864.
[50] J.K. Gregory, D.C. Clary, K. Liu, M.G. Brown, R.J. Saykally, Science 275 (1997) 814.
[51] B.J. Costa Cabral, R.C. Guedes, R.S. Pai-Panandiker, C.A.N. de Castro, Phys. Chem. Chem. Phys. 3 (2001) 4200.